Sulfaphenazole Derivatives as Tools for Comparing Cytochrome P450 2C5 and Human Cytochromes P450 2Cs: Identification of a New High Affinity Substrate Common to Those Enzymes[†]

Cristina Marques-Soares,[‡] Sylvie Dijols,[‡] Anne-Christine Macherey,[‡] Michael R. Wester,[§] Eric F. Johnson,[§] Patrick M. Dansette,[‡] and Daniel Mansuy*,[‡]

Laboratoire de Chimie et Biochimie Pharmacologiques et Toxicologiques, UMR 8601 CNRS, Université Paris V, 45 Rue des Saints-Pères, 75270 Paris Cedex 06, France, and Department of Molecular and Experimental Medicine, The Scripps Research Institute, 10550 North Torrey Pines Road MEM-255, La Jolla, California

Received December 20, 2002; Revised Manuscript Received March 25, 2003

ABSTRACT: The inhibitory effects of a series of sulfaphenazole (SPA) derivatives were studied on two modified forms of rabbit liver cytochrome P450 2C5 (CYP2C5), CYP2C5dH, and structurally characterized CYP2C5/3LVdH and compared to the previously described effects of these compounds on human CYP2C8, 2C9, 2C18, and 2C19. SPA and other negatively charged compounds that potently inhibit CYP2C9 had very little effect on CYP2C5dH, whereas neutral, N-alkylated derivatives exhibited IC50 values between 8 and 22 μM. One of the studied compounds, **4**, that derives from SPA by replacement of its NH_2 substituent with a methyl group and by N-methylation of its sulfonamide moiety, acted as a good substrate for all CYP2Cs used in this study. Hydroxylation of the benzylic methyl of **4** is the major reaction catalyzed by all of these CYP2C proteins, whereas hydroxylation of the *N*-phenyl group of **4** was observed as a minor reaction. CYP2C5dH, 2C5/3LVdH, 2C9, 2C18, and 2C19 are efficient catalysts for the benzylic hydroxylation of **4**, with K_m values between 5 and 13 μM and k_{cat} values between 16 and 90 min^{-1}. The regioselectivity observed for oxidation of **4** by CYP2C5/3LVdH was easily interpreted on the basis of the existence of two different binding modes of **4** characterized in the experimentally determined structure of the complexes of CYP2C5/3LVdH with **4** described in the following paper [Wester, M. R. et al. (2003) *Biochemistry 42,* 6370−6379].

In mammals, most metabolic oxidations of xenobiotics such as drugs are catalyzed by cytochromes P450 of the first three families (CYP1, 2, and 3)[1] (*1*, *2*). Efforts to interpret or predict various problems that may occur with some drugs, such as drug−drug interactions or consequences of genetic polymorphism, have led to routine characterization of the specific human P450 enzymes that metabolize new drug candidates. It would also be useful to know which structural factors are important for substrate recognition by the various human P450s. However, the structural basis for the metabolic diversity exhibited by mammalian drug metabolizing P450-dependent monooxygenases is poorly understood, and it is still difficult to predict the substrate specificities and metabolic products for these enzymes.

In this regard, the recent report (*3*) of the first structure of a mammalian, microsomal P450 from rabbit liver, CYP2C5, is an important step toward the understanding of substrate recognition by drug-metabolizing P450s. Since the publication of the structure, several 3-D models of different mammalian P450s have been constructed on the basis of the CYP2C5 X-ray structure by molecular modeling techniques (*4*−*9*). Such an approach would be greatly facilitated if one could start from the X-ray structures of complexes of CYP2C5 with various substrates (or inhibitors) resembling those of the other drug-metabolizing P450s of interest. However, very few substrates of CYP2C5 have been reported so far (*10*, *11*).

Recently, we synthesized several derivatives of sulfaphenazole, SPA, which is a potent and relatively selective inhibitor of human liver CYP2C9 ($K_i = 0.3$ μM) and used these derivatives as tools for comparing the active sites of the human P450s of the 2C subfamily, CYP2C8, 2C9, 2C18, and 2C19 (*12*−*14*), which are the most closely related human enzymes to CYP2C5. The present study was undertaken to compare the interactions of the SPA derivatives with CYP2C5 to those with the human CYP2Cs. The objectives of the study were 2-fold: (i) to obtain the first data on the differences of behavior of CYP2C5 and human CYP2Cs toward recognition of a given series of compounds and (ii) to find new high affinity substrates of CYP2C5 and determine the first X-ray structure of CYP2C5 complexed

[†] This work was supported by CNRS and French Minister of Research (D.M.) and by the NIH Grant GM31001 (E.F.J.). C.M.S. was recipient of a CNRS-Aventis fellowship.

* To whom correspondence should be addressed. Tel.: 33 1 42 86 21 87. Fax: 33 1 42 86 83 87. E-mail: Daniel.Mansuy@biomedicale.univ-paris5.fr.

[‡] Laboratoire de Chimie et Biochimie Pharmacologiques et Toxicologiques.

[§] The Scripps Research Institute.

[1] Abbreviations: Ac, $COCH_3$; CYP, cytochrome P450; DMSO, dimethyl sulfoxide; EDTA, ethylenediamine tetraacetic acid; HEPES, *N*-(2-hydroxyethyl)piperazine-*N*′-(2-ethanesulfonic acid); HPLC, high-performance liquid chromatography; MS, mass spectrometry; HPLC-ESI/MS, HPLC coupled with electron spray ionization mass spectrometry; MS/MS-CID, collision induced dissociation mass spectrometry; SPA, sulfaphenazole.

10.1021/bi027391+ CCC: $25.00
Published on Web 05/08/2003

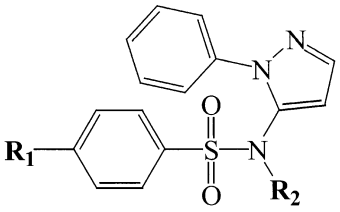

FIGURE 1: General formula of the SPA derivatives used in this study. For SPA, $R_1 = NH_2$ and $R_2 = H$. For compound **4**, also named DMZ in the following paper (*15*), $R_1 = R_2 = CH_3$.

with a molecule that is also well-recognized by human CYP2Cs. This study allowed us to identify a new substrate of CYP2C5 that is also a substrate for the four human CYP2Cs. The X-ray structure of the complex of this substrate with CYP2C5 is described in the following paper (*15*).

MATERIALS AND METHODS

Chemicals. All chemicals used were of the highest quality commercially available. SPA, progesterone, and diclofenac were provided by Sigma (St. Quentin Fallaviers, France).

Physical Measurements. UV−vis spectra were recorded on an Aminco DW-2 apparatus modified by Olis Inc (Bogart, GA). ^{1}H NMR spectra were recorded at 27 °C on a Bruker ARX-250 instrument (Wissenbourg, France); chemical shifts are reported downfield from $(CH_3)_4Si$, and coupling constants are in Hz. The following abbreviations: s, bs d, t, and m are used for singlet, broad singlet, doublet, triplet, and multiplet, respectively. Elemental analyses were carried out at the Centre Regional de Microanalyse, Paris. High-pressure liquid chromatography coupled to electron spray ionization mass spectrometry (HPLC−ESI/MS) was done on a Thermofinnigan ion trap instrument LCQ Advantage equipped with a Surveyor HPLC system (Thermofinnigan, Les Ulis, France).

Synthesis of SPA Derivatives. Compounds **1**−**5** were synthesized as described previously (*13*, *14*). *4-Hydroxymethyl-N-methyl-N-(2-phenyl-2H-pyrazol-3-yl)-benzene sulfonamide, **6**.* 4-(Methylsulfinyl)benzyl acetate and acetic acid 4-chlorosulfonyl-benzyl ester were prepared as previously described (*16*, *17*). This arylsulfonyl chloride (870 mg, 3.5 mmol) was dissolved in dry CH_2Cl_2 (17 mL) and pyridine (0.29 mL, 3.6 mmol). 570 mg (3.6 mmol) of 2-phenyl-2*H*-pyrazol-3-ylamine (*18*) were added. After 48 h at room temperature, the reaction mixture was extracted with aqueous Na_2CO_3. The aqueous phase was washed with CH_2Cl_2, neutralized with concentrated HCl, and extracted with CH_2Cl_2. The organic phase was dried over $MgSO_4$. Chromatography on silica gel (CH_2Cl_2-EtOAc 7%) gave 300 mg of acetic acid 4-(2-phenyl-2*H*-pyrazol-3-sulfamoyl)-benzyl ester (23% yield); mp 134−135 °C. ^{1}H NMR ($CDCl_3$) δ 7.65 (d, 2H, $J = 8.4$), 7.54 (d, 1H, $J = 1.9$), 7.40−7.34 (m, 5H), 7.10−7.06 (m, 2H), 6.25 (d, 1H, $J = 1.9$), 5.14 (s, 2H), 2.13 (s, 3H). Methyl iodide (0.04 mL, 0.64 mmol) was added to a solution of this compound (150 mg, 0.4 mmol) in 1 mL of anhydrous DMF containing 70 mg of Na_2CO_3. After 20 h at room temperature, DMF was evaporated, and the residue was dissolved in CH_2Cl_2. The organic phase was washed with water and dried over $MgSO_4$. After purification by column chromatography (SiO_2, CH_2Cl_2-EtOAc 5%), 140 mg of product was obtained in a 91% yield; mp 97−98 °C. ^{1}H NMR ($CDCl_3$) δ 7.69 (d, 2H, $J = 8.3$), 7.58−7.53 (m, 3H), 7.48−7.40 (m, 5H), 5.90 (d, 1H, $J = 1.9$), 5.18 (s, 2H), 3.06 (s, 3H), 2.15 (s, 3H). This product (120 mg, 0.31 mmol) was stirred for 1 h at room temperature under argon in 6 mL of EtOH and 2 mL of 0.2 N NaOH. Water was added, and the solution was extracted with CH_2Cl_2. The organic phase was dried over $MgSO_4$ and evaporated. Crystallization from diethyl ether gave compound **6** in 94% yield; mp 131−132 °C. ^{1}H NMR ($CDCl_3$) δ 7.68 (d, 2H, $J = 8.3$), 7.57 (m, 3H), 7.51−7.37 (m, 5H), 5.87 (d, 1H, $J = 1.9$), 4.81 (d, 2H, $J = 5.3$), 3.04 (s, 3H), 1.92 (t, 1H, OH, $J = 5.3$). Anal. calcd. for $C_{17}H_{17}N_3O_3S$: C, 59.46; H, 4.99; N, 12.24. Found: C, 59.29; H, 4.99; N, 12.23.

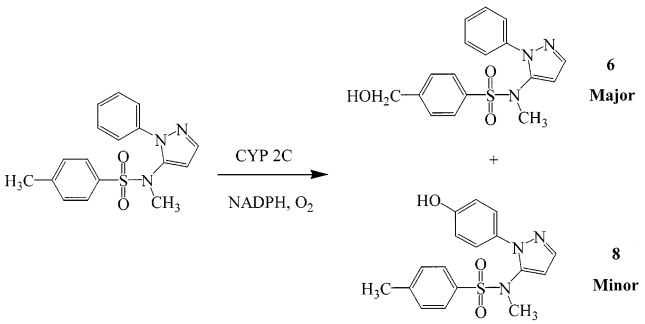

FIGURE 2: Structure of the primary metabolites formed upon oxidation of **4** by CYP2C5dH and human CYP2Cs.

*4-Formyl-N-methyl-N-(2-phenyl-2H-pyrazol-3-yl)-benzene sulfonamide, **7**.* Oxidation of **6** (2.5 mg) with MnO_2 (20 mg) in acetone (1 mL) at room temperature for 24 h afforded 2 mg of aldehyde **7**. ^{1}H NMR ($CDCl_3$) δ 10.12 (s, 1H), 8.04 (d, 2H, $J = 8.4$), 7.85 (d, 2H, $J = 8.4$), 7.57 (d, 2H, $J = 8$), 7.53 (bs, 1H), 7.5−7.3 (m, 3H), 5.88 (bs, 1H), 3.11 (s, 3H). HPLC-ESI/MS, $[M + H]^+ = 342$. HPLC-ESI/MS/MS-CID, $m/e = 173$.

*N-[2-(4-Hydroxy-phenyl)-2H-pyrazol-3-yl]-4,N-dimethyl-benzenesulfonamide, **8**.* The synthesis of 4-methyl-*N*-[2-(4-methoxy-phenyl)-2*H*-pyrazol-3-yl]-benzenesulfonamide was previously described (*13*). Methyl iodide (0.022 mL, 0.35 mmol) was added to a solution of 4-methyl-*N*-[2-(4-methoxy-phenyl)-2*H*-pyrazol-3-yl]-benzenesulfonamide (85 mg, 0.25 mmol) in 0.5 mL of anhydrous DMF containing 40 mg of Na_2CO_3. After 15 h at room temperature, DMF was evaporated, and the residue was dissolved in CH_2Cl_2. The organic phase was washed with water and dried over $MgSO_4$. After purification by column chromatography (SiO_2, CH_2Cl_2-EtOAc 5%), 82 mg of product was obtained in a 93% yield; mp 142−143 °C. ^{1}H NMR ($CDCl_3$) δ 7.59 (d, 2H, $J = 8$), 7.53 (d, 1H, $J = 1.4$), 7.47 (d, 2H, $J = 8.8$), 7.30 (d, 2H, $J = 8$), 6.95 (d, 2H, $J = 8.8$), 5.84 (d, 1H, $J = 1.4$), 3.84 (s, 3H), 3.00 (s, 3H), 2.44 (s, 3H). This product (40 mg, 0.11 mmol) was heated with pyridine hydrochloride (500 mg) at 175 °C for 1 h. The reaction mixture was cooled, and water was added. The product was extracted with CH_2Cl_2, dried over $MgSO_4$, and purified by TLC (SiO_2, 1 mm; CH_2Cl_2-EtOAc, 12%). Compound **8** was obtained in a 44% yield and crystallized from CH_2Cl_2-cyclohexane; mp 211−212 °C. ^{1}H NMR ($CDCl_3$) δ 7.59 (d, 2H, $J = 8$), 7.54 (d, 1H, $J = 1.2$), 7.36 (d, 2H, $J = 8.8$), 7.31 (d, 2H, $J = 8$), 6.81 (d, 2H, $J = 8.8$), 5.93 (s, OH), 5.85 (d, 1H, $J = 1.2$), 3.01 (s, 3H), 2.45 (s, 3H). Anal. calcd. for $C_{17}H_{17}N_3O_3S$: C, 59.46; H, 4.99; N, 12.24. Found: C, 59.30; H, 5.08; N, 12.18.

Yeast Transformation, Cell Culture, and Preparation of the Yeast Microsomal Fraction. The expression system used for human liver P450s was based on a yeast strain W(R)-fur1 previously described (*19*) in which yeast cytochrome P450 reductase was overexpressed. Transformation by the pYeDP60 vector containing one of the human liver CYP2C8, 2C9, 2C18, and 2C19 cDNAs was then performed according to a general construction method of yeast strain W(R)fur1 expressing various human liver cytochromes P450s (*20*, *21*). Yeast culture and preparation of microsomes were performed using previously described techniques (*22*). Microsomes were suspended in a 50 mM Tris buffer pH = 7.4, containing 1 mM EDTA and 20% glycerol (v/v), aliquoted, frozen under liquid N_2, and stored at −80 °C until use. P450 contents of yeast microsomes were 40, 90, 40, and 20 pmol of P450/mg protein for CYP2C8, 2C9, 2C18, and 2C19, respectively. The microsomal P450 content was determined according to the method of Omura and Sato (*23*). The protein content was determined by the Lowry et al. procedure using bovine serum albumin as a standard (*24*).

Expression and Purification of CYP2C5dH, CYP2C5/3LVdH, and P450 Reductase from Escherichia coli. CYP2C5dH and CYP2C5/3LVdH were constructed from the CYP2C5 cDNA, expressed, and purified as described previously (*11*). The average specific contents of the preparations of P450 2C5dH and 2C5/3LVdH were 16.5 and 15.4 nmol/mg protein, respectively. Human liver P450 reductase was isolated following its expression in *E. coli* and purified as described previously (*11*). The activity of the purified reductase preparation was determined spectrophotometrically (*25*). The specific activity was 26 units/mg protein (meaning that 26 μmol of cytochrome *c* was reduced in 1 min by 1 mg of protein) and corresponds to 2 units/nmol protein.

Study of Substrate Binding to CYP2C5dH or CYP2C5/3LVdH by Difference Visible Spectroscopy. Substrate dependent spectral changes were monitored by difference visible absorption spectra recorded at room temperature. Purified CYP2C5dH or CYP2C5/3LVdH was dissolved in a 50 mM HEPES buffer, pH = 7.6, containing 1.5 mM $MgCl_2$ and 0.1 mM EDTA, to obtain a P450 concentration of 0.3−0.8 μM. The solution was equally divided between two 150 μL quartz cuvettes (1 cm path length), and a baseline was recorded. Aliquots (0.3−0.5 μL) of DMSO solutions containing the studied compound were added to the sample cuvette; the same volume of DMSO was added to the reference cuvette. The difference spectra were recorded between 380 and 520 nm (*26*).

Inhibition of CYP2C5dH-Catalyzed 21-Hydroxylation of Progesterone by SPA Derivatives. The catalytic system consisted of a mixture of purified CYP2C5dH (25 pmol) and purified human P450 reductase (0.75 units) in 50 μL of 50 mM HEPES buffer pH = 7.6, containing 1 mM $MgCl_2$ and 0.1 mM EDTA, that was incubated in ice for 10 min. In the study of substrate oxidation by CYP2C5dH (or CYP2C5/3LVdH), this mixture was then diluted to reach a final incubation volume of 350 μL of the same buffer containing the substrate and placed in a shaking-bath at 37 °C. The reaction was initiated (t_0 = 0 min) by the addition of an NADPH-generating system (1 mM $NADP^+$, 10 mM glucose 6-phosphate, and 2 units of glucose 6-phosphate dehydrogenase/mL). At t_0 and regularly thereafter, aliquots (80 μL) were taken, and the reaction was quickly stopped by the treatment with 50 μL of cold CH_3CN/CH_3COOH (10/1). After centrifugation (10 000*g*, 5 min in an Eppendorf centrifuge), the supernatants were analyzed by HPLC performed on a Xterra RP18 column (Waters, Saint-Quentin en Yvelines, France) (5 μm, 4.6 × 250 mm) with a linear gradient from an aqueous solution of $(NH_4)HCO_3$ (25 mM) to CH_3CN over 30 min at a flow rate of 1 mL/min. Diclofenac (2 μM) was used as a standard, and products were detected at 240 nm. Under these conditions, the 21-hydroxylation of progesterone exhibited k_{cat} and K_m values of 12 min^{-1} and 4 μM, respectively, in agreement with previously reported data (*11*).

In the study of the inhibitory effects of SPA derivatives, identical incubation mixtures containing 20 μM progesterone and various concentrations of inhibitors (between 2 and 250 μM) were employed to measure the IC50 values.

*CYP2C-Catalyzed Oxidations of Compound **4**: Analysis of the Products by HPLC-ESI/MS.* Oxidation of **4** by CYP2C5dH or CYP2C5/3LVdH was performed under conditions similar to those described in the previous paragraph either with 300 μM **4** and a 60 min incubation or with 20 μM **4** and a 6 min incubation. Reactions were stopped by adding 150 μL of CH_3CN, and the crude mixture was directly analyzed by HPLC-ESI/MS.

Oxidation of **4** by human CYP2Cs was done by incubating 300 μM **4** in 1 mL of 10 mM phosphate buffer pH 7.4 containing microsomes prepared from W(R)fur1 yeast expressing each human CYP2C (0.1−0.2 μM) and the NADPH-generating system described above for 60 min at 28 °C. Acetic acid (20 μL) was added at the end of the incubation to precipitate the proteins, and the samples were centrifuged at 1000*g*. The supernatants were loaded on a 1 mL Oasis column (Waters, Saint-Quentin en Yvelines, France), rinsed with 1 mL of H_2O, and eluted with 1 mL of methanol. The eluate was concentrated to a 250 μL volume and used for HPLC-ESI/MS analysis.

HPLC-ESI/MS employed a Browlee C4 column (5 μM, 2 × 100 mm) (Touzard et Matignon, Vitry-sur-Seine, France). The samples (10 or 20 μL) were injected with the automatic sample injector, and substrates, products, and standards were separated using a linear gradient from A (formic acid, 10 mM ammonium acetate (5:995)) to B (CH_3CN, H_2O, formic acid, 900:100:5) in 16 min, at a flow rate of 200 μL/min. Source tuning set up was sheat gas 45, auxiliary gas 2, spray voltage 5 kV, capillary temperature 275 °C, capillary voltage 3 V, and tube lens offset −10 V. MS and MS/MS-CID (mass spectrometry collision induced dissociation) spectra were obtained in scan and single ion monitoring (SIM) mode. The diode array detector was set from 200 to 400 nm. The instrument was calibrated by using an equimolar mixture of authentic **4**, **6**, **7**, and **8**. HPLC retention times of these four compounds were 12.3, 10.6, 11.4, and 11.8 min, respectively. Their molecular peak (MS) and main fragment (MS/MS-CID) were observed at *m*/*e* = 328, 344, 342, and 344 and 173, 173, 173, and 189, respectively.

*CYP2C-Catalyzed Benzylic Hydroxylation of **4**: Kinetic Analysis.* Oxidation of **4** by CYP2C5dH or CYP2C5/3LVdH was performed under the conditions described above for 21-hydroxylation of progesterone with the following modifications. The amounts of P450 and reductase preincubated for 10 min at 0 °C in 50 μL of HEPES buffer were 4.5 pmol

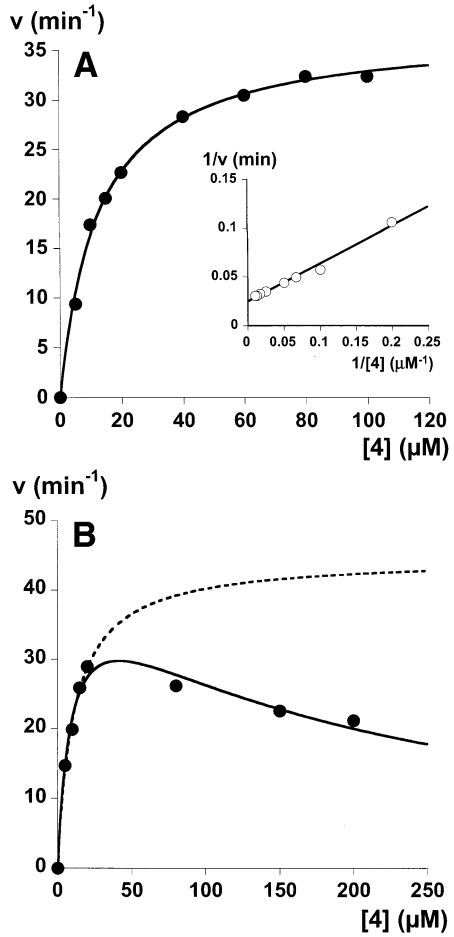

FIGURE 3: Kinetics of benzylic hydroxylation of **4** catalyzed by CYP2C9 (A) or CYP2C5/3LVdH (B). Initial rates (in nmol of **6** × nmol P450^{-1} min^{-1}), as a function of [**4**] (in μM), were determined as indicated in Materials and Methods. Inset: Lineweaver−Burk plot of the data of panel A. Panel B (—): Curve fitting the experimental data according to the classical kinetic model of enzymatic reactions involving inhibition by excess substrate (*27*) based on the expression $v = k_{cat}'[S]/(K_m' + [S](1 + [S]/K_s'))$ and leading to apparent $K_m' = 10 \pm 2$ μM, $k_{cat}' = 40 \pm 5$ min^{-1} and apparent $K_s' = 180 \pm 40$ μM. (- - -): Curve that would correspond to a classical Michaelis behavior by only taking into account the data obtained for substrate concentrations lower than 20 μM.

and 0.14 units, respectively, and the final P450 concentration in the incubations with **4** was 0.02 μM. Oxidation of **4** by human CYP2Cs was done by using microsomes of W(R)fur1 yeast expressing each human CYP2C (0.02−0.1 μM) in 50 mM Tris buffer pH 7.4 containing 1 mM EDTA, 8% glycerol (v/v), and the NADPH-generating system described above, at 28 °C. Reactions were stopped by addition of a cold CH_3CN/CH_3COOH (10:1) mixture (50 μL). After centrifugation (10 000*g*, 5 min in an Eppendorf centrifuge), the supernatants were analyzed by HPLC performed on a Hypersil MOS column (Thermofinnigan, Les Ulis, France) (5 μm, 4.6 × 250 mm) using a linear gradient from A (H_2O) to B ($CH_3CN/CH_3OH/H_2O$ (7/2/1)) for 12 min at a flow rate of 1 mL/min. The formation of product **6** was followed at 235 nm.

Some CYP2C reactions, such as those of CYP2C8 and CYP2C9 (Figure 3A), followed classical Michaelis−Menten kinetics; the corresponding K_m and k_{cat} values were derived from analysis of Lineweaver−Burk or Michaelis plots using Kaleidagraph 3.0. For other CYP2C reactions, such as those

Table 1: Comparison of the Inhibitory Effects of Various SPA Derivatives (see Figure 1) toward CYP2C5dH and Human CYP2Cs[a]

			IC50 (μM)				
compd	R_1	R_2	2C5dH	2C8	2C9	2C18	2C19
SPA	NH_2	H	>150[b]	130	0.6	60	>500[b]
1	CH_3	H	>150[b]	220	0.6	170	100
2	NH_2	$(CH_2)_2CH_3$	22	8	55	8	250
3	NH_2	$(CH_2)_3CH_3$	8	4	50	6	60
4	CH_3	CH_3	20	180	10	12	20
5	*m*-nitro-phenyl	$(CH_2)_4OH$	15	>250[b]	15	4	>200[b]

[a] IC50 values for the inhibition of human CYP2Cs are those reported in two previous articles (*13*, *14*). The values were determined by using a substrate concentration equal to the K_m of the followed reaction. In the case of CYP2C5dH, 21-hydroxylation of progesterone by the purified recombinant protein in the presence of human P450 reductase was used to test the inhibitors; details are described in Materials and Methods. For that reaction, 20 μM substrate was used (five times the K_m of CYP2C5dH-catalyzed 21-hydroxylation of progesterone, which was 4 ± 1 μM in our conditions) because of analytical constraints. Values are the means from three experiments. [b] CYP2C activity higher than 50% control activity at the indicated inhibitor concentration.

of CYP2C18 and 2C19, the data could well be fitted with a classical model of enzymatic kinetics involving an inhibition by excess substrate, according to (*27*):

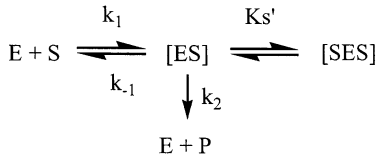

In this model, $v = k_{cat}'[S]/(K_m' + [S](1 + [S]/K_s'))$, v being the initial rate, [S] the concentration of substrate, k_{cat}' and K_m' the apparent kinetic constants, and K_s' an apparent equilibrium constant.

RESULTS AND DISCUSSION

Interaction of Various SPA Derivatives with CYP2C5: Comparison with Human CYP2Cs. Two proteins derived from CYP2C5 were used in the following studies. The first one, CYP2C5dH, resulted from the substitution of a short, positively charged N-terminal sequence for the native transmembrane, leader sequence of CYP2C5 to improve its solubility, and by addition of a 4-histidine tag to the C-terminus to facilitate purification of the protein (*11*). The second one, CYP2C5/3LVdH, resulted from additional amino acid substitutions that alter the surface of the protein in the vicinity of the F helix to further improve the solubility and monodispersity of the protein in high salt buffers (*11*). The X-ray structure previously published was that of CYP2C5/3LVdH (*3*).

SPA, an especially high affinity inhibitor of CYP2C9 (K_i = 0.3 μM (*13*)), failed to inhibit the CYP2C5-catalyzed hydroxylation of progesterone in a significant manner (Table 1). Compound **1**, a selective inhibitor of CYP2C9 that is as potent as SPA (K_i = 0.4 μM (*13*)) and that derives from SPA by replacement of its NH_2 substituent with a methyl group, also failed to significantly inhibit CYP2C5dH. In contrast, compounds **2** and **3** that derive from SPA by N-alkylation of its sulfonamide function were good inhibitors of CYP2C5dH with IC50 values of 22 and 8 μM, respectively (Table 1). The large increase of the affinity of SPA

derivatives for CYP2C5dH after the N-alkylation of the sulfonamide function is similar to that previously observed in the case of CYP2C8 and 2C18 (Table 1). On the other hand, N-alkylation of SPA, which suppresses the negative charge of SPA, led to a dramatic decrease of the affinity toward CYP2C9. Thus, contrary to CYP2C9 that better recognizes anionic SPA derivatives, CYP2C5dH exhibits a much better affinity for neutral, N-alkylated compounds such as **2**−**5**.

Other neutral, N-alkylated derivatives of SPA, in which the NH_2 group has been replaced with a methyl or a meta-nitrophenyl substituent (compounds **4** and **5**, respectively) also exhibited a good affinity for CYP2C5dH (Table 1). If one assumes that compounds **2**−**5** are competitive inhibitors of CYP2C5dH-catalyzed hydroxylation of progesterone, the K_i values estimated from the IC50 values (Table 1) are in the μM range (1.5−4 μM). This assumption was determined to be true in the case of compound **2** that acted as a competitive inhibitor with an experimentally determined K_i value of 4 ± 1 μM. If one compares the IC50 values measured for CYP2C5dH, 2C8, 2C9, 2C18, and 2C19 as a function of the structure of the SPA derivative, CYP2C18 is the human CYP2C that displays behavior most similar to CYP2C5dH. In the case of CYP2C8 and CYP2C19, at least one SPA derivative exhibits a behavior that significantly differs from that seen with CYP2C5dH. As the results of Table 1 indicated that compound **4** (called DMZ in the following paper (*15*)) was well-recognized not only by CYP2C5dH but also by the four human CYP2Cs, the potential for this compound to act as a substrate for all of these enzymes was studied as described in the following experiments.

Oxidation of Compound 4 by CYP2C5dH and Human CYP2Cs (Figure 2). Aerobic incubation of **4** with recombinant, purified CYP2C5dH in the presence of purified human cytochrome P450 reductase and an NADPH-generating system, for 1 h at 37 °C, led to the formation of a major metabolite, as shown by HPLC (see Materials and Methods). Analysis of the structure of this metabolite by MS coupled to HPLC (HPLC-ESI/MS) and ^{1}H NMR spectroscopy after isolation by preparative HPLC indicated that it was derived from the hydroxylation of the benzylic methyl group of **4** (molecular peak at $[M + H]^+ = 344$, as compared to 328 for **4**; replacement in ^{1}H NMR of the signal at 2.44 ppm of the benzylic methyl group of **4** with a signal at 4.81 ppm corresponding to a benzylic CH_2 group). An authentic sample of the corresponding metabolite, **6**, was then synthesized according to a procedure described in Materials and Methods and completely characterized by elemental analysis, MS, and ^{1}H NMR spectroscopy. Its spectroscopic characteristics and HPLC retention time were found to be identical to those of the major metabolite of **4**.

Two minor metabolites were also formed during the CYP2C5dH-dependent oxidation of **4**. The less polar one, **7**, showed a molecular peak at $[M + H]^+ = 342$ in HPLC-ESI/MS and a fragment in MS/MS coupled to HPLC (HPLC-ESI/MS/MS-CID) at $m/e = 173$. MS/MS spectra of compound **4** and its metabolite **6**, which were performed under identical conditions, displayed fragments at the same mass that corresponds to the *N*-phenyl-aminopyrazolyl part of the molecule, which is not modified during the oxidation of **4** to produce **6**, or the minor, less polar metabolite, **7**. These data strongly suggested that this minor metabolite was the aldehyde derived from the further oxidation of the alcohol function of **6.** Accordingly, incubation of **6** under the conditions used previously for oxidation of **4** led to a major metabolite that exhibited MS and MS/MS-CID characteristics identical to those of **7**. Moreover, an authentic sample of the aldehyde **7** was synthesized from oxidation of **6** by MnO_2 and characterized by MS and ^{1}H NMR spectroscopy (see Materials and Methods). Its HPLC retention time and MS characteristics were also found to be identical to those of metabolite **7**.

Table 2: Regioselectivity of the Hydroxylation of **4** by CYP2C5dH and Human CYP2Cs[a]

P450	2C5dH	2C8	2C9	2C18	2C19
8/**6** ratio	0.004	0.008	<0.001	<0.001	0.03

[a] Conditions of the reactions are described in Materials and Methods, using [**4**] = 300 μM. The **8**/**6** ratio was determined by HPLC−ESI/MS spectrometry, on the basis of the intensities of the corresponding ions, after calibration using a mixture of authentic samples of **6** and **8**. Values are the means from three experiments.

The second minor metabolite, **8**, formed in the CYP2C5dH-dependent oxidation of **4**, appeared to be an isomer of **6**, as shown by its molecular peak in HPLC-ESI/MS at $m/e = 344$. Its MS/MS spectrum showed a fragment corresponding to the *N*-phenyl-aminopyrazolyle part of the molecule at $m/e = 189$. This suggested that **8** was derived from hydroxylation of this part of compound **4,** most likely at the chemically favored para position. The corresponding compound was synthesized according to a procedure described in Materials and Methods and completely characterized by elemental analysis, MS, and ^{1}H NMR spectroscopy. The authentic compound exhibited a HPLC retention time and mass spectral characteristics identical to those of the minor metabolite **8**.

Similar experiments were performed to study the oxidation of **4** by human CYP2C8, 2C9, 2C18, and 2C19. For this purpose, microsomes from yeast strain W(R)fur1 expressing each CYP2C were used in the presence of an NADPH-generating system and O_2 (see Materials and Methods). CYP2C9 led to the almost exclusive formation of metabolite **6** (30% conversion under the used conditions); the formation of **7** and **8** was under our detection limit (<0.06%). In a more general manner, **6** was by far the major metabolite with CYP2C5dH and all human CYP2Cs, as it represented between 90 and 100% of the total metabolites. Phenol **8** was only a very minor metabolite when compared to **6**, the **8**/**6** ratio varying between 0 for CYP2C9 and 2C18 to 0.004 for CYP2C5dH, 0.008 for CYP2C8, and 0.03 for CYP2C19 (Table 2). Aldehyde **7** was also a minor metabolite, and its amounts in the reaction mixture varied between 0 and 8% of the total metabolites as a function of the nature of the P450 2C involved and the conditions.

Kinetics of Benzylic Hydroxylation of 4 by CYP2C5dH, CYP2C5/3LVdH, and human CYP2Cs. From the aforementioned results, CYP2C5dH and the human CYP2Cs all catalyzed the oxidation of **4** yielding the benzylic alcohol **6** as a major product. To further compare those CYP2C enzymes, we measured the kinetic constants of the corresponding oxidations. Two kinds of curves were observed for the dependence of the initial rate on substrate concentration

Table 3: Kinetic Characteristics of the Benzylic Hydroxylation of **4** Catalyzed by CYP2C5dH, 2C5/3LVdH, and Human CYP2Cs[a]

	CYP					
	2C5dH[b]	2C5/3LVdH[b]	2C8	2C9	2C18[b]	2C19[b]
K_m (μM)	13 ± 8	10 ± 2	40 ± 5	12 ± 1	5 ± 3	8 ± 3
k_{cat} (min^{-1})	90 ± 20	40 ± 5	4 ± 1	35 ± 5	40 ± 8	16 ± 2
k_{cat}/K_m	7	4	0.1	3	8	2

[a] Conditions described in Materials and Methods. Values are mean ± SD from three to six experiments. [b] For the reactions showing an inhibition by excess substrate at concentrations higher than 20 μM (see Figure 3B for instance), apparent k_{cat} and K_m values were calculated on the basis of data obtained for concentrations of **4** lower than 20 μM.

(Figure 3). CYP2C8 and 2C9-catalyzed benzylic hydroxylations of **4** exhibited a classical Michaelis behavior (Figure 3A), with K_m values of 40 ± 5 and 12 ± 1 μM and k_{cat} values of 4 ± 1 and 35 ± 5 min^{-1}, respectively (Table 3). Data obtained with other CYP2C reactions could be described by a classical model of enzymatic kinetics involving inhibition by excess substrate with the binding of a second molecule of substrate to the enzyme−substrate complex that leads to a nonproductive entity (*27*). Such a situation was observed in the case of the oxidation of **4** by CYP2C5/3LVdH (Figure 3B) under the conditions described in Materials and Methods. It was also found in oxidations of **4** catalyzed by microsomes of yeast expressing CYP2C18 and 2C19. Supplementary experiments remain to be done to determine the molecular origin of this phenomenon. In that regard, several experiments have been performed to examine whether one of the reaction products, **6**, **7**, or **8**, could act as a strong inhibitor of the CYP2C5 enzymes. None of them led to such strong inhibitory effects, and they were characterized by IC50 values higher than those found for **4** itself (data not shown). Other experiments showed that increasing, by a factor of 4, the concentrations of CYP2C5/3LVdH and of human P450 reductase in the preincubation performed to reconstitute the CYP2C5/3LVdH monooxygenase prevented the inhibition of the enzyme at high concentrations of the substrate. This suggests that differences in the reconstitution of the enzyme with the reductase could contribute to the stability of the protein in the presence of high concentrations of the substrate. The k_{cat} and K_m values determined using this procedure did not differ significantly from the estimates obtained using the initial conditions for reconstitution (data not shown). These results indicate that the conditions used for reconstitution of the monooxygenase play a role in the appearance of inhibition by excess substrate kinetics for CYP2C5/3LVdH.

Apparent K_m and k_{cat} values calculated from the inhibition by excess substrate model (*27*) were very similar to those that were calculated from the Lineweaver−Burk plots derived from rates observed for substrate concentrations lower than 20 μM. Thus, apparent K_m and k_{cat} values of 13 ± 8, 10 ± 2, 5 ± 3, and 8 ± 3 μM and 90 ± 20, 40 ± 5, 40 ± 8, and 16 ± 2 min^{-1} were calculated for CYP2C5dH, 2C5/3LVdH, 2C18, and 2C19, respectively (Table 3). These data show that the two modified CYP2C5 (CYP2C5dH and 2C5/3LVdH) exhibit almost identical K_m values for benzylic hydroxylation of **4**. In fact, all the experiments that we have performed to compare the properties of these two proteins for their inhibition by sulfaphenazole derivatives or their oxidation of **4** gave very similar results. These data also show that **4** is an interesting common substrate of CYP2C5 and human CYP2Cs. All these CYP2Cs, except CYP2C8, hydroxylate **4** with a high catalytic efficiency, as shown by k_{cat}/K_m values between 2 and 8 min^{-1} μM^{-1} (Table 3), which are relatively high for the CYP2C subfamily (*28*). CYP2C8 is markedly less efficient than the other CYP2Cs as shown by its k_{cat}/K_m value that is 1−2 orders of magnitude lower.

The relatively good affinity of **4** for CYP2C5dH is suggested by the K_m value of its hydroxylation, 13 μM (Table 3), which is in the same range as the IC50 of its inhibition of CYP2C5-catalyzed hydroxylation of progesterone (Table 1). Supplementary experiments were performed to determine the effects of **4** on the visible spectrum of CYP2C5/3LVdH. Addition of increasing amounts of **4** to this hemoprotein led to the appearance of a visible difference spectrum characterized by a peak at 393 nm and a trough at 421 nm (data not shown). This type I difference spectrum is usually observed after binding of a substrate to a P450 active site in close proximity to the heme resulting in the transition of the heme iron from its low spin hexacoordinated to high spin pentacoordinated state (*26*). The intensity of this difference spectrum indicated that about 20% of the hemoprotein was involved in this spin state change. The corresponding plot of $1/\Delta A_{(393-421\ nm)}$ as a function of 1/[**4**] for concentrations of **4** compatible with its solubility in 50 mM HEPES buffer, pH 7.6 ([**4**] < 120 μM), was a straight line from which a K_s value of 20 ± 5 μM could be calculated. This value is similar to the K_m value determined for the CYP2C5/3LVdH-catalyzed benzylic hydroxylation of **4**.

CONCLUSION

CYP2C5 proteins recognize neutral, N-alkylated SPA derivatives such as **2**−**5** well. One of those compounds, **4** (called DMZ in the following paper (*15*)), is the first good CYP2C5 substrate that is also a good substrate for human CYP2Cs. Hydroxylation of **4** by those 2C enzymes mainly occurs at the benzylic methyl group, leading to **6**, but also at the *N*-phenyl ring, leading to **8** as a minor product. Formation of **6** and **8** could be interpreted either by the existence of two modes of substrate binding to the active site of CYP2C5 or by a great mobility of **4** in this active site. The structure of CYP2C5/3LVdH complexed with **4** (M. R. Wester et al., accompanying paper (*15*)) shows that the former interpretation is the correct one. The corresponding data show that, in the first binding mode, the benzylic methyl group of **4** is located at a very short distance, 4.4 Å, from the iron. In the second binding mode, **4** points its *N*-phenyl substituent toward the iron; however, the phenyl ring is positioned further (5.9 Å) from the iron. These differences in the positioning of the substrate are consistent with the observed regioselectivity of CYP2C5-catalyzed oxidation of **4**, which greatly favors benzylic hydroxylation (**8**/**6** = 0.004, Table 2). Interestingly, the regioselectivity of **4** hydroxylation by human CYP2Cs is different. CYP2C9 and CYP2C18 almost exclusively produce metabolite **6**, whereas CYP2C8 and especially CYP2C19 yield higher relative amounts of **8** (**8**/**6** = 0.008 and 0.03, respectively, Table 2). Further experiments are required to determine the origin of these differences.

The structure of the CYP2C5/3LVdH−**4** complexes (*15*) also showed that there is additional space available in the

substrate binding site to accommodate SPA derivatives with larger R_1 and R_2 substituents. This could explain the good affinities of compounds **2**, **3**, and **5**, which bear larger R_2 substituents (and R_1 substituent in the case of **5**) than compound **4** (Table 1).

REFERENCES

1. Koymans, L., Den Kelder, G. M., Koppele, T., J. M., and Vermeulen, N. P. E. (1993) *Drug Metab. Rev. 25*, 325−387.
2. Guengerich, F. P. (1995) in *Cytochrome P450: Structure, Mechanism, and Biochemistry* (Ortiz de Montellano, P. R., Ed.) pp 473−535, Plenum Press, New York.
3. Williams, P. A., Cosme, J., Sridhar, V., Johnson, E. F., and McRee, D. E. (2000) *Mol. Cell 5*, 121.
4. Spatzenegger, M., Wang, Q. M., He, Y. Q., Wester, M. R., Johnson, E. F., and Halpert, J. R. (2001) *Mol. Pharmacol. 59*, 475−484.
5. Afzelius, L., Zamora, I., Ridderstrom, M., Andersson, T. B., Karlen, A., and Masimirembwa, C. M. (2001) *Mol. Pharmacol. 59*, 909−919.
6. Tsao, C. C., Wester, M. R., Ghanayem, B., Coulter, S. J., Chanas, B., Johnson, E. F., and Goldstein, J. A. (2001) *Biochemistry 40*, 1937−1944.
7. De Groot, M. J., Alex, A. A., and Jones, B. C. (2002) *J. Med. Chem. 45*, 1983−1993.
8. Wang, Q. M., and Halpert, J. R. (2002) *Drug Metab. Dispos. 30*, 86−95.
9. Melet, A., Assrir, N., Jean, P., Lopez-Garcia, M. P., Marques-Soares, C., Jaouen, M., Dansette, P. M., Sari, M. A., and Mansuy, D. (2003) *Arch. Biochem. Biophys. 409*, 80−91.
10. Trant, J. M., Lorence, M. C., Johnson, E. F., Shackleton, C. H. L., Mason, J. I., and Estabrook, R. W. (1990) *Biochemistry 87*, 9756−9760.
11. Cosme, J., and Johnson, E. F. (2000) *J. Biol. Chem. 275*, 2545−2553.
12. Mancy, A., Dijols, S., Poli, S., Guengerich, P., and Mansuy, D. (1996) *Biochemistry 35*, 16205−16212.
13. Ha-Duong, N. T., Marques-Soares, C., Dijols, S., Sari, M. A., Dansette, P. M., and Mansuy, D. (2001) *Arch. Biochem. Biophys. 394*, 189−200.
14. Ha-Duong, N. T., Dijols, S., Marques-Soares, C., Minoletti, C., Dansette, P. M., and Mansuy, D. (2001) *J. Med. Chem. 44*, 3622−3631.
15. Wester, M. R., Johnson, E. F., Marques-Soares, C., Dansette, P. M., Mansuy, D., and Stout, D. C. (2003) *Biochemistry 42*, 6370−6379.
16. Samanen, J. M., and Brandeis, E. (1988) *J. Org. Chem. 53*, 561−569.
17. De Vleeschauwer, M., and Gauthier, J. Y. (1997) *Synlett*. 375−377.
18. Schmidt, P., and Druey, J. (1958) *Helv. Chim. Acta 41*, 306−309.
19. Truan, G., Cullin, C., Reisdorf, P., Urban, P., and Pompon, D. (1993) *Gene 125*, 49−55.
20. Urban, P., Truan, G., Bellamine, A., Laine, R., Gautier, J. C., and Pompon, D. (1994) *Drug Metab. Drug Interact. 11*, 169−200.
21. Pompon, D., Louerat, B., Bronine, A., and Urban, P. (1996) *Methods Enzymol. 272*, 51−64.
22. Bellamine, A., Gautier, J. C., Urban, P., and Pompon, D. (1994) *Eur. J. Biochem. 225*, 1005−1013.
23. Omura, T., and Sato, R. (1964) *J. Biol. Chem. 239*, 2379−2385.
24. Lowry, O. H., Rosebrough, N. J., Farr, A. L., and Randall, R. J. (1951) *J. Biol. Chem. 193*, 265−275.
25. Peterson, J. A., and Mock, D. M. (1975) *Anal. Biochem. 68*, 545−553.
26. Jefcoate, C. R. (1978) *Methods Enzymol. 52*, 258−279.
27. Cornish-Bowden, A. (1995) *Fundamentals of enzyme kinetics*, Portland Press, Brookfield, VT.
28. Goldstein, J. A., and de Morais, S. M. (1994) *Pharmacogenetics 4*, 285−299.

BI027391+